Heat Assisted Magnetic Recording Air Bearing Simulations that Account for the Lateral Air Temperature Variation

Joanna E. Bechtel* and David B. Bogy

Department of Mechanical Engineering, Computer Mechanics Laboratory, University of California, Berkeley, California 94720, USA

Abstract

Heat assisted magnetic recording (HAMR) is a promising hard disk drive technology to reach 4 Tb/in^2 storage densities. However HAMR introduces significant thermal considerations that must be accounted for in air bearing simulations; the laser spot on the recording bit and heat dissipated into the slider by the laser delivery system result in boundary wall temperatures that are several hundred degrees Celsius above ambient. Since the air bearing film between the slider and disk is non-isothermal, the local air properties should be used in the lubrication equation that governs the pressure generation. A molecular gas lubrication equation for the air bearing that accounts for large temperature variation along the film was previously proposed by Fukui and Kaneko, but they presented scant detail in their derivation, and it has yet to be applied to a HAMR hard disk drive. This paper explains in considerable detail the generalized lubrication equation and also implements it into a realistic 2D simulation using a production slider with approximate HAMR conditions. The minimum flying height increases substantially while the pitch and roll are inappreciably affected. Thermal creep flow is negligible compared with Poiseuille and Couette flows, and it can be omitted consideration. The sensitivity of the read/write transducer would be affected by the large increase in minimum fly height; therefore the TFC design process must consider these variations due to thermal variations in the air bearing.

1 Introduction

The magnetic recording industry widely views heat-assisted magnetic recording (HAMR) as a technology to achieve 4 Tb/in^2 storage densities in hard disk drives [1, 2]. Novel components such as a laser delivery system integrated into the slider and a special magnetic medium have been developed to the point that researchers are performing first-generation

*Corresponding author: jobechtel@berkeley.edu

HAMR recording demonstrations [3]. As the HAMR technology progresses toward commericialization, thermal management along with other practical issues still need to be addressed [4]. One significant thermal issue is the heat dissipated into slider body by the laser delivery system and the resulting several nanometers of distortion [2]. Design of transducer geometry, location, and surrounding material as well as ABS design can control peak temperature and heat flow [5]. As designs are iterated to minimize thermal issues, a lubrication equation that sufficiently captures important air bearing behavior under HAMR conditions needs to be implemented into a full slider simulation tool.

Fukui and Kaneko's molecular gas lubrication (MGL) equation [6] is widely used for air bearing simulations of traditional (non-HAMR) hard disk drives. In these implementations, the air bearing can be assumed isothermal and therefore thermal creep flow is absent; the heater in a thermal fly height (TFC) slider only heats the ABS surface $\mathcal{O}(10^{\circ}\mathrm{C})$ above ambient in a confined location so an isothermal assumption is reasonable. For these isothermal air bearings, comparison with Direct Simulation Monte Carlo (DSMC) results verified the MGL equation in non-contact situations down to nanometer-scale minimum fly heights [7]. However HAMR introduces significant thermal considerations that must be accounted for in air bearing simulations; the laser spot on the recording bit and heat dissipated into the slider by the laser delivery system result in boundary wall temperatures that are several hundred degrees Celsius above ambient. Fukui and Kaneko presented a form of the MGL equation including thermal creep flow for large temperature difference between the boundary wall and the ambient characteristic temperature [8]. To date, no publication has reported an application of this equation to a HAMR hard disk drive.

In this paper, Section 2 explains the derivation of the MGL equation with thermal creep for large temperature differences with some added explanation not included in Fukui and Kaneko's papers. In Section 3, this governing equation for the HAMR air bearing is implemented into a two dimensional simulation for a production air bearing surface (ABS) design with plausible slider temperature and protrusion profiles. Section 4 presents the simulation results, and Section 5 discusses implications of the report findings. A summary and concluding remarks are in Section 6.

2 A Generalized Lubrication Equation for Non-Isothermal Systems

The classical Reynolds equation for compressible fluids governs the pressure generation in a lubricating gas film. Quoted in many texts (e.g. [9, pg. 60]), this continuum regime equation applies to viscous Newtonian fluids if the temperature gradient is assumed negligible and the pressure is assumed to be independent of the film thickness coordinate. However, the technique of integrating the conservation equation across a film thickness is not dependent on a continuum or lubrication assumption; it can be used for a rarefied gas

as well. After applying Leibnitz's rule to interchange the integration and differentiation operators, we obtain the integrated conservation equation as

$$\frac{\partial(\rho h)}{\partial t} + \frac{\partial}{\partial x}\left[\int_0^h (\rho u)dz\right] + \frac{\partial}{\partial y}\left[\int_0^h (\rho v)dz\right] = 0 \tag{1}$$

ρ is the fluid local density, h is the local fluid film thickness, and u and v are the local fluid velocity components in the x and y directions. This mass conservation equation across the film thickness can be re-written in terms of mass flow rate per unit length, q:

$$\frac{\partial(\rho h)}{\partial t} + \frac{\partial q_x}{\partial x} + \frac{\partial q_y}{\partial y} = 0 \tag{2}$$

The mass flow rates q_x and q_y are the mass fluxes in the planar x and y directions integrated across the film.

$$\begin{aligned} q_x &= \int_0^h (\rho u)dz \\ q_y &= \int_0^h (\rho v)dz \end{aligned} \tag{3}$$

After accurate expressions for mass flow rates for a rarefied gas film are determined, those mass flow rates can be inserted into Equation 2.

The Boltzmann equation governs fluidic and thermal gas transport for a dilute gas such as an HDD air bearing over the entire Knudsen number regime and for non-equilibrium conditions [10]. Macroscopic quantities such as mass flow rate are related to the velocity distribution function of particles, the quantity found by Boltzmann equation, through various integrals. Rarefied gases are composed of three fundamental flows: pressure driven Poiseuille flow, shear driven Couette flow, and boundary temperature gradient driven thermal creep (transpiration) flow. Scientists derived non-dimensional expressions for these elemental flow rates by solving a simplified Boltzmann equation that employs the linearized BGK model for the collision integral and idealistic gas-solid interactions at the boundaries [11, 12]. These flow rate expressions are valid for flows with small pressure and temperature gradients and apply over the entire rarefaction range—continuum to free molecular flow. The flow rates depend on the local Knudsen number and the surface properties of both bounding surfaces, represented by the surface accomodation coefficient α. The slider studied in this report had a maximum spacing in its base etch of ≈ 25500 nm (Kn $\approx 0.0025 < 0.01$, continuum regime) and the minimum fly height of only ≈ 2 nm (Kn $\approx 32 > 10$, free-molecular flow); hence the HAMR air bearing experiences the entire rarefaction range.

Fukui and Kaneko (FK) [6] inserted expressions for the dimensional rarefied gas mass flow rates into Equation 2. Considering only one flow direction (x) for brevity, they ob-

tained

$$\frac{\partial(\rho h)}{\partial t} + \frac{\partial}{\partial x}\left(\frac{\rho U h}{2} Q_C - \frac{h^2}{\sqrt{2RT}}\frac{dp}{dx} Q_P + \frac{p h^2}{T\sqrt{2RT}}\frac{dT_w}{dx} Q_T\right) = 0 \tag{4}$$

U is the boundary velocity, T is the local fluid temperature, p is the local fluid pressure, $\frac{dT_w}{dx}$ is the boundary wall temperature gradient, and R is the specific gas constant (universal gas constant divided by the molecular mass). Q_C, Q_P, and Q_T are the non-dimensional flow rates for Couette, Poiseuille, and thermal creep flow. For symmetric boundaries that have the same surface properties and therefore the same accomodation coefficients, Q_C is always unity. In this paper, the slider and disk surfaces are assumed to be symmetric with a perfectly diffuse surface, $\alpha = 1$. To make this generalized lubrication equation directly comparable to the classical Reynolds equation (e.g. in [9, pg. 60]), FK normalized the non-dimensional Poiseuille and thermal creep flow rates by the Poiseuille flow rate in continuum flow, $Q_{con} = D/6 = \sqrt{\pi}/(12\mathrm{Kn})$. In the limit as $\mathrm{Kn} \to 0$, their equation reduces to a non-dimensionalized form of the classical Reynolds equation.

Cercignani was a pioneer in the area of rarefied gas dynamics, obtaining numerical and approximate analytical solutions valid for the entire Knudsen number regime ($0 \leq \mathrm{Kn} < \infty$). He applied an approximate variational principle method to calculate Poiseuille and Couette flow rates [13], which closely matched his earlier finite difference numerical solutions to the linearized Boltzmann equation [14] but were less computationally expensive. Cercignani used a non-dimensionlization convention for the Poiseuille rarefied gas flow rate [14]; the flow rate dependence on pressure (or Knudsen number, since mean free path changes with pressure) for a fixed pressure gradient and plate separation can be non-dimensionalized by the quantity $-h^2\frac{dp}{dx}$. The negative sign makes the non-dimensional flow rate quantity positive; the fluid flows from high pressure to low pressure, so the direction of mass velocity is in the opposite direction of the pressure gradient. Cercignani used molecular velocity units of $\sqrt{2RT}$ in all rarefied gas analyses, so to convert the non-dimensional Poiseuille flow rate to SI units, the non-dimensionalizing quantity is $-\frac{h^2}{\sqrt{2RT}}\frac{dp}{dx}$.

The Poiseuille flow rate non-dimensionalization and solution method were later analogously used by Loyalka for thermal creep flow [15]; he non-dimensionalized the mass flow due to thermal creep by the term

$$\frac{1}{2}\sqrt{2RT_0}\rho h^2 \frac{1}{T_0}\frac{dT}{dx} = \frac{p h^2}{T\sqrt{2RT_0}}\frac{dT}{dx} \tag{5}$$

The subscript 0 presumably is a reference quanity. The ideal gas law has been used in this equality. This is exactly the same form of the Poiseulle flow non-dimensionalization quantity used by Cercignani:

$$-\frac{1}{2}\sqrt{2RT_0}\rho h^2 \frac{1}{p_0}\frac{dp}{dx} = -\frac{\rho h^2}{\rho_0\sqrt{2RT_0}}\frac{dp}{dx} = -\frac{h^2}{\sqrt{2RT_0}}\frac{dp}{dx} \text{ if } \rho \approx \rho_0 \tag{6}$$

FK also adopted these non-dimensionalizations in their work on the generalized Reynolds equation.

Though the general form of the Poiseuille and thermal creep flow rate non-dimensionalization quantities are standard, one finds that the temperature and pressure—local or reference gas temperature and pressure values or the boundary wall temperature—is not consistent between authors or even publications of the same author. Cercignani's work with Poiseuille and Couette flow was isothermal so the temperature was obvious. Loyalka was consistent in most publications using the non-dimensionalization in the previous paragraph; ρ and h are presumably local values. FK defined the thermal creep flow rate as [6]

$$Q_T \equiv \frac{q_T}{\frac{ph^2}{T_0\sqrt{2RT_0}}\frac{dT_w}{dx}} \tag{7}$$

and also as [8]

$$Q_T \equiv \frac{q_T}{\frac{ph^2}{T_w\sqrt{2RT_w}}\frac{dT_w}{dx}} \tag{8}$$

In this report, local air property values and gradients and the local spacing are used in the non-dimensionalization of the mass flow rates. The local value of the appropriate flow-inducing gradient is also used: the local pressure gradient for Poiseuille flow and the local boundary temperature gradient for thermal creep. For the x direction,

$$Q_P \equiv \frac{q_{P,x}}{\frac{h^2}{\sqrt{2RT}}\frac{dp}{dx}} \qquad Q_T \equiv \frac{q_{T,x}}{\frac{ph^2}{T\sqrt{2RT}}\frac{dT_w}{dx}} \tag{9}$$

With these definitions and using the Q_{con} normalization proposed by FK, the one dimensional, steady state integrated mass conservation equation becomes

$$\frac{d}{dx}\left(q_{C,x} + q_{P,x} + q_{T,x}\right) = \frac{d}{dx}\left(\frac{\rho U h}{2} - \frac{h}{\sqrt{2RT}}\frac{dp}{dx}\overline{Q}_P\frac{D}{6} + \frac{ph^2}{T\sqrt{2RT}}\frac{dT_w}{dx}\overline{Q}_T\frac{D}{6}\right) = 0 \tag{10}$$

where the relative non-dimensional mass flow rates are defined according to [6]

$$\overline{Q}_P = \frac{Q_P}{Q_{con}} \qquad \overline{Q}_T = \frac{Q_T}{Q_{con}} \tag{11}$$

According to the hard elastic sphere model, the mean free path λ is related to the viscosity μ as [16]

$$\mu \approx \sqrt{\frac{2RT}{\pi}}\rho\lambda = \frac{2}{\sqrt{\pi}}\frac{p}{\sqrt{2RT}}\lambda \tag{12}$$

Using this relation, the inverse Knudsen number D can be expressed as

$$D = \frac{\sqrt{\pi}}{2\mathrm{Kn}} = \frac{\sqrt{\pi}h}{2\lambda} = \frac{ph}{\mu\sqrt{2RT}} \tag{13}$$

The lubrication equation [Equation 10] is non-dimensionalized according to

$$\begin{aligned} P &= \frac{p}{p_0} \qquad X = \frac{x}{L} \\ \overline{T} &= \frac{T}{T_0} \qquad \overline{\mu} = \frac{\mu}{\mu_0} \\ H &= \frac{h}{h_0} \end{aligned} \tag{14}$$

The subscript 0 always denotes ambient or characteristic values. L is the characteristic length, the slider length in the case of an air bearing simulation. Using Equations 13 and 14, Equation 10 becomes

$$\frac{d}{dX}\left[\frac{1}{\overline{\overline{T}}}\left(\Lambda_0 PH - \frac{PH^3}{\overline{\mu}}\overline{Q}_P\frac{dP}{dX} + \frac{P^2H^3}{\overline{\mu}\overline{T}}\overline{Q}_T\frac{d\overline{T}_w}{dX}\right)\right] = 0 \tag{15}$$

where the bearing number in the x direction, which is constant for a particular head-disk system with a constant rotational speed, is defined as

$$\Lambda_0 = \frac{6LU\mu_0}{p_0 h_0^2} \tag{16}$$

This is the same equation as Fukui and Kaneko's molecular gas lubrication equation for large temperature differences [8] except for the bearing number. They defined the bearing number in terms of local viscosity $\Lambda = \frac{6LU\mu}{p_0 h_0^2}$. Since the viscosity changes with temperature and hence location on the slider, we choose here to define the bearing number in terms of constant characteristic quantities. The change in viscosity is put with the Poiseuille and thermal creep flow terms.

When numerically solving the Equation 15, the slider and disk temperature distributions are assumed to be known and are inputs to the simulation. These bounding surface temperatures are used to estimate the air bearing temperature. $\overline{T} = \overline{T}(x, y)$ refers to the non-dimensionalized air temperature which along with other air properties is assumed to be constant through the air bearing thickness. The temperature of the air at a particular point (x, y) under the slider is estimated to be the average of the disk and slider temperature at that point. Since the air temperature will lie somewhere in this range, it's a reasonable first approximation.

$$\overline{T}(x, y) = \frac{1}{2}\left(\frac{T_{slider}(x, y) + T_{disk}(x, y)}{T_0}\right) \tag{17}$$

Similarly the non-dimensionalized temperature gradient of the boundary, the driving force for thermal creep flow, is the average of the non-dimensionalized slider and disk temperature gradients at that point. Fukui and Kaneko made this arithmetic average suggestion for instances when the top and bottom bounding surfaces have different temperature gradients [6].

$$\frac{d\overline{T}_w}{dX} = \frac{1}{2}\frac{L}{T_0}\left(\frac{dT_{slider}}{dx} + \frac{dT_{disk}}{dx}\right) \tag{18}$$

The air viscosity, a function of temperature, is calculated from the estimated air bearing temperature using Sutherland's Formula for the viscosity of a gas. Sutherland proposed a model that considered gas molecules to be hard spheres and added a weak attractive force between molecules that decays rapidly with distance; his hypothesis is adequate over a wide range of temperatures for many gases, including air [17, pg. 154-157], [18, pg. 27-28]. The detail of the Chapman and Cowling viscosity expression [Equation 12] is unnecessary for routine calculations because temperature has a strong effect while pressure has a moderate effect on viscosity.

$$\overline{\mu} = \frac{\mu}{\mu_0} = \left(\frac{T}{T_0}\right)^{3/2}\left(\frac{T_0 + C}{T + C}\right) \tag{19}$$

where μ_0 is a known viscosity at a known absolute temperature and Sutherland's constant C is fit to the data. For air, the reference viscosity at the reference temperature $T_0 = 273.15$ K is $\mu_0 = 1.71e-5$ kg/m/s and the empirically fitted constant is $C = 110.4$ K [18, pg. 810].

The non-dimensional mass flow rates Q_P and Q_T are functions of the Knudsen number and the surface accommodation coefficients for the slider and disk. For simplicity, the surface accommodation coefficients for both bounding surfaces are assumed to be 1; the surfaces reflect gas molecules diffusely regardless to the direction of incidence. Therefore only the dependence of the flow rates on the Knudsen number needs to be considered. According to kinetic theory, the mean free path of a hard elastic sphere in an ideal Maxwellian gas with diameter d and number density n is [17, pg. 113]

$$\lambda = \frac{1}{\sqrt{2}\pi d^2 n} = \frac{m}{\sqrt{2}\pi d^2 \rho} = \frac{mRT}{\sqrt{2}\pi d^2 p} \tag{20}$$

m is the mass of the ideal gas molecule. The local in mean free path λ at a certain temperature T and pressure p is then

$$\frac{\lambda}{\lambda_0} = \frac{T}{T_0}\frac{p_0}{p} \tag{21}$$

Since Kn=$\frac{\lambda}{h}$,

$$\frac{\mathrm{Kn}}{\mathrm{Kn}_0} = \frac{T}{T_0}\frac{p_0}{p} \tag{22}$$

The local mass flow rates can be evaluated at the local pressure and temperature values.

$$Q_P(\mathrm{Kn}) = Q_P\left(\mathrm{Kn}_0\frac{\overline{T}}{\overline{P}}\right) \qquad Q_T(\mathrm{Kn}) = Q_P\left(\mathrm{Kn}_0\frac{\overline{T}}{\overline{P}}\right) \tag{23}$$

3 Simulation of Flying Attitude

Static simulations using the steady state generalized lubrication equation [Equation 15] were carried out using the ABS design shown in Figure 1 and the protrusion profile shown in Figure 2. The sliders dimensions are 0.851 mm long by 0.751 mm wide. The protrusion from the zero plane ABS surface is defined over various rectangles (0.5 mm, 0.2 mm) to (0.851 mm, 0.5 mm), and it has a maximum protrusion of 20 nm at the location (0.8264 mm, 0.3514 mm). This large protrusion profile approximates a potential protrusion due to the heater and laser delivery system. Three different radii were considered, inner, middle, and outer diameter positions. The radial locations and the accompanying skew angles are listed in Table 1. Also listed in the table are the steady state flying attitudes for the case of an isothermal slider and disk. All simulations in this report are for a disk rotational speed of 5400 RPM. Ambient air properties are 25°C air at sea level. All simulations assume a perfectly flat disk with no roughness.

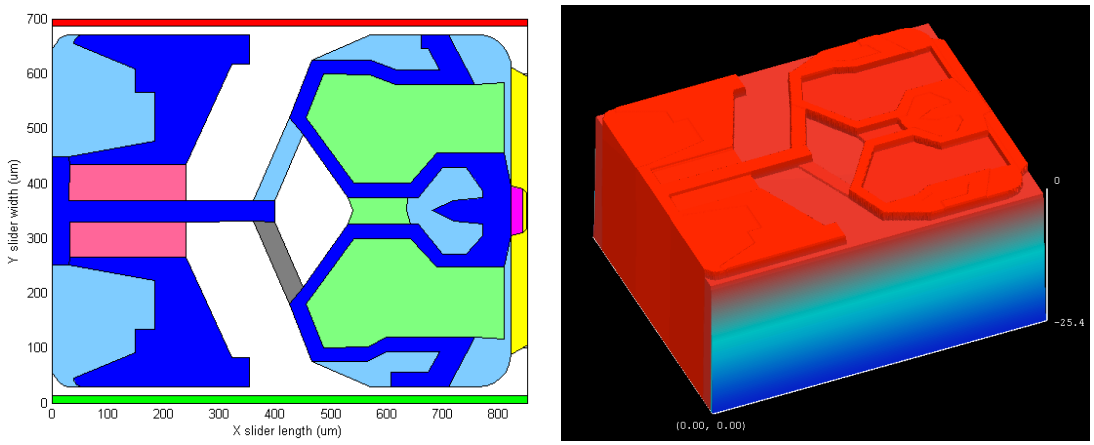

(a) ABS Design (b) 3D ABS Geometry

Figure 1: Air bearing surface (ABS) design used for all simulations.

Simulations with different ABS temperature profiles were tested to determine how the flying attitude changes. These temperature profiles vary in size of the heated area and maximum temperature (100°C, 200°C, and 300°C). All maximum temperatures are assumed to occur at (0.8212 mm, 0.3489 mm), which is close to the peak protrusion location

of (0.8264 mm, 0.3514 mm). For each maximum temperature we examine confined heated areas and expansive heated areas. The confined temperature profiles are representative of a laser delivery system that dissipates heat to a relatively small area of the slider body. The expansive temperature profiles represent a highly dissipative laser delivery system that heats up a relatively large portion of the slider. Contour plots of the ABS temperature profiles for the different maximum temperatures and heat spot areas are overlaid onto the rails in Figure 3. The same protrusion profile is used for all ABS temperature profiles in the simulation results reported here. Admittedly, a different ABS temperature profile indicates a different applied TFC power, and hence a different protrusion profile. However the focus of this report is to show the difference in simulation results when using the isothermal MGL equation vs. the large temperature difference MGL equation and how the effects change with ABS temperature profile.

Although the disk will be heated above its Curie temperature, reaching 200-600°C depending on the media used, the recording area per bit of $(25\text{ nm})^2$ [2] is negligible in a full slider simulation. The hot spot on the disk could only be captured in one node, and it would have no effect on the slider flying attitude.

The in-house air bearing simulation tool CMLAir iteratively solves a discretized finite volume formulation of Equation 15 with a V-cycle multigrid method to find the pressure profile that balances the user defined load. Detailed descriptions of the discretized governing equation and solution algorithm can be found in [19, 20]. To speed up computation, databases for Q_P and Q_T over a wide range of Knudsen numbers are evaluated in the preprocessing section of the simulation. During the multigrid solution operation, the database is interpolated to find the local flow rate values. Reference [20] describes how the Q_P and Q_T databases are populated using Cercignani's [13] and Loyalka's [21] variational solutions with Chebyshev polynomial expansions for the Abramowitz functions [22]. The slider's

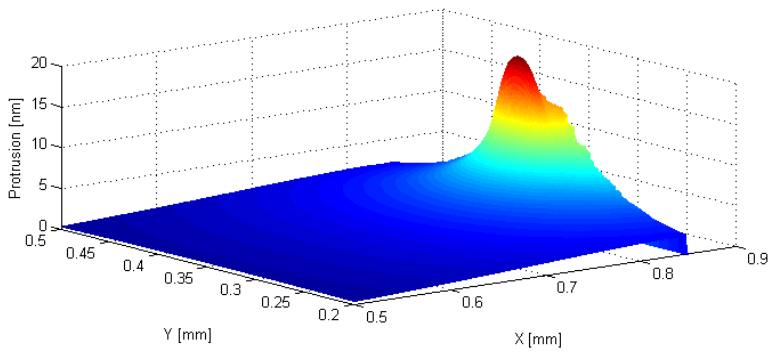

Figure 2: Protrusion profile used for all simulations. The protrusion below the zero plane ABS surface is defined over the rectangle (0.5 mm, 0.2 mm) to (0.851 mm, 0.5 mm) and has a maximum protrusion of 20 nm.

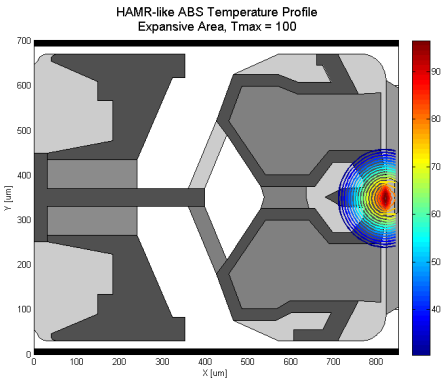

(a) $T_{max} = 100°\text{C}$ with an expansive heat area

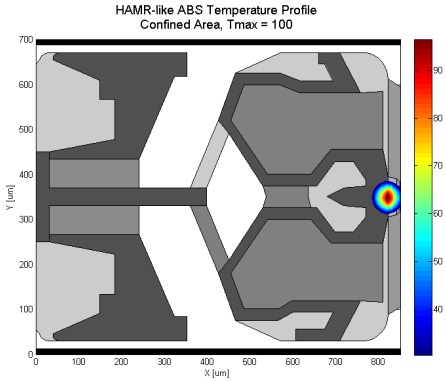

(b) $T_{s,max} = 100°\text{C}$ wiqth a confined heat area

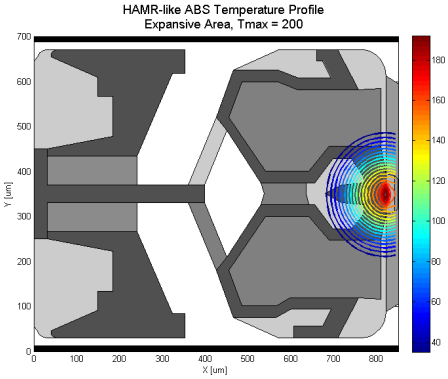

(c) $T_{s,max} = 200°\text{C}$ with an expansive heat area

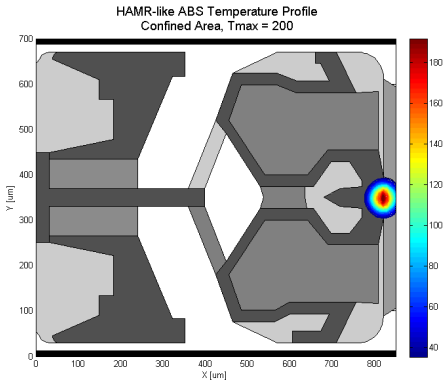

(d) $T_{s,max} = 200°\text{C}$ with a confined heat area

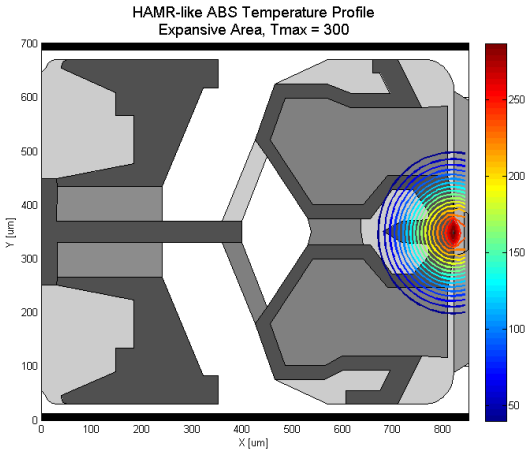

(e) $T_{s,max} = 300°\text{C}$ with an expansive heat area

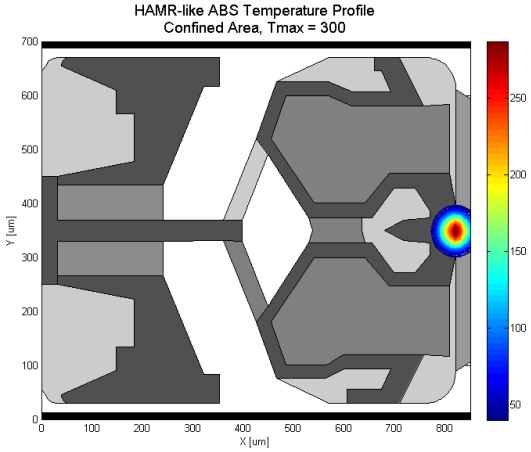

(f) $T_{s,max} = 300°\text{C}$ with a confined heat area

Figure 3: ABS temperature profiles and the relation to the ABS rails.

Table 1: Static flying attitude solutions three radii for the case of an isothermal slider. min FH is the minimum fly height between the slider and disk. nom FH is the nominal fly height at the trailing edge center location.

Radius (mm)	Skew (deg)	RPM	min FH (nm)	nom FH (nm)	Pitch (μrad)	Roll (μrad)
14.53	-14.769	5400	2.16271	18.0245	63.7889	-2.7841
22.215	0.943	5400	2.41924	18.1378	69.6114	2.21038
29.924	11.891	5400	2.1697	18.0453	62.9754	2.69646

flying attitude parameters of pitch, roll, and minimum flying height are calculated for the equilibrium pressure profile. The minimum fly height is defined as the minimum physical spacing between the slider's air bearing surface and the assumed smooth disk surface. Pitch and roll have the usual flying dynamics definitions.

4 Simulation Results

The steady state minimum fly height results for all ABS temperature profiles, including an isothermal ABS at ambient temperature, are shown in Figure 4. The minimum fly height value and percent change compared with the isothermal slider simulation are plotted. The minimum fly height increases with increasing maximum ABS temperature and extent of the heated ABS region. In all cases, the change in minimum fly height is greater at the middle radial location than the outer or inner radii. For the expansive heated ABS region simulations, the change in minimum fly height was significant, from 5% to almost 45% increase in minimum fly height across the three radii. The percent change was less significant for the confined ABS heated region simulations, but still it is non-negligible for the 200°C and 300°C cases in which the percent change in minimum fly height ranged from 6.5% to 10.7% at the middle radii.

The value and percent change of pitch are shown in Figure 5. The pitch decreases slightly with increasing maximum ABS temperature and extent of the heated ABS region in almost all cases. As with the minimum and nominal fly height solutions, the greatest amount of change occurs at the middle radius while the inner and outer radii show about the same about of change in pitch angle. The confined ABS heated region cases show a small change of -1% to 0.25% for all temperature and radial positions. The extensive ABS heated region simulations showed more decrease in pitch angle, from -0.1% to -3.2%.

The roll angle changes very little between ABS temperature profile cases and all the values lie practically on top of each other [Figure 6].

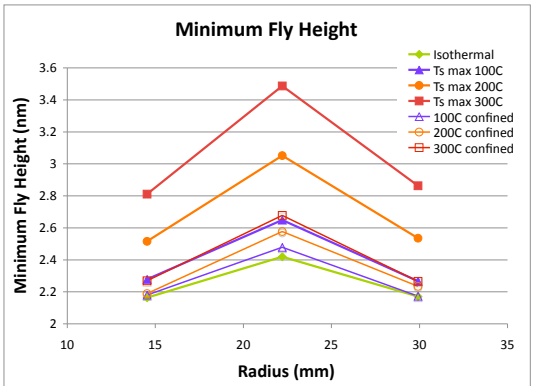

(a) Minimum Fly Height

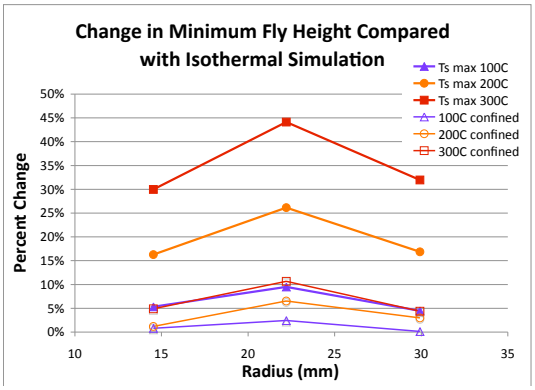

(b) Percent Change

Figure 4: Steady state minimum fly height absolute values and percent change compared with the isothermal steady state flying attitude simulation.

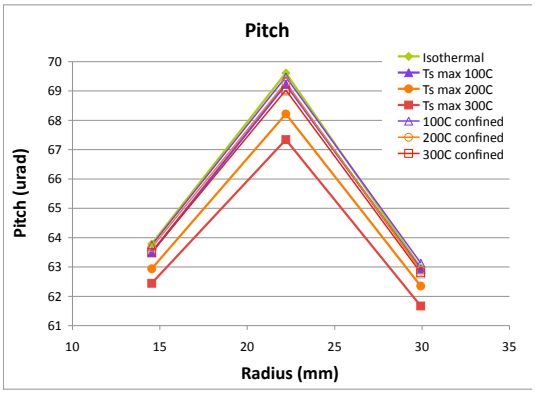

(a) Pitch

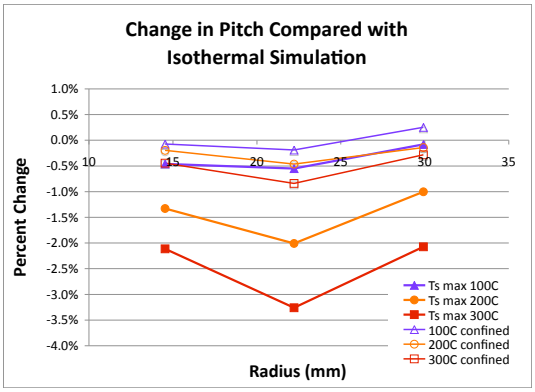

(b) Percent Change

Figure 5: Steady state pitch value at the center of the trailing edge (TEC) and percent change compared with the isothermal steady state flying attitude simulation.

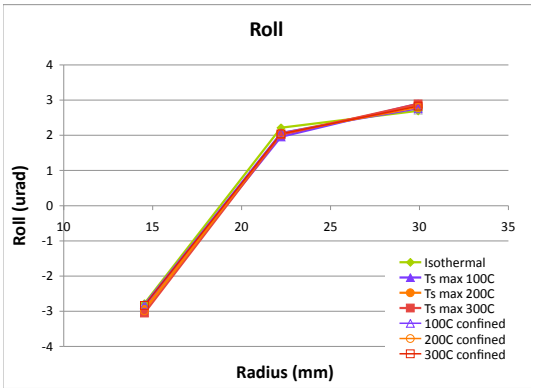

Figure 6: Steady state roll remains approximately constant.

Table 2: Static flying attitude solution for the expansive 300°C slider temperature profile [Figure 3(e)] with and without thermal creep. min FH is the minimum fly height between the slider and disk. nom FH is the nominal fly height at the trailing edge center location.

	Radius (mm)	Skew (deg)	min FH (nm)	nom FH (nm)	Pitch (μrad)	Roll (μrad)
With Thermal Creep	14.53	-14.769	2.81037	18.6975	62.4399	-3.05099
	22.215	0.943	3.48675	19.2788	67.3404	2.01413
	29.924	11.891	2.86248	18.7644	61.668	2.88699
Without Thermal Creep	14.53	-14.769	2.81161	18.6985	62.435	-3.05573
	22.215	0.943	3.48021	19.2711	67.3575	2.01528
	29.924	11.891	2.86593	18.768	61.6615	2.93008

A simulation omitting the thermal creep term from the generalized lubrication equation was performed to determine the importance of the thermal creep effect on the steady state flying attitude of the slider. The expansive 300°C slider temperature profile [Figure 3(e)] is the most extreme temperature condition tested, so thermal creep should have the most effect for this case. Slider attitude parameters differ between the cases with and without thermal creep only at the third decimal place [Table 2]. The percent change in attitude parameters ranged from -0.19% to 1.49% [Table 3].

5 Discussion

A physical reasoning of the increased minimum fly height results shown in Figure 4 is as follows. Recall that the slider ABS temperature along with the isothermal disk temperature

Table 3: Percent change in slider flying attitude parameters when thermal creep is omitted for the expansive 300°C slider temperature profile.

Radius (mm)	Skew (deg)	min FH change	nom FH change	Pitch change	Roll change
14.53	-14.769	0.04%	0.01%	-0.01%	0.16%
22.215	0.943	-0.19%	-0.04%	0.03%	0.06%
29.924	11.891	0.12%	0.02%	-0.01%	1.49%

are used to estimate the air temperature at a particular point. So if the slider ABS temperature is greater than ambient temperature, the air at that location is estimated to be hotter than ambient. Air is assumed to be an ideal gas in the generalized lubrication equation, and according to the ideal gas law, pressure is proportional to temperature. Thus an increase in temperature over an area means an increase in pressure. The air exerts a greater lift force on the slider and thus it flies higher with a larger minimum spacing.

The pitch simulation results also agree with expectations. Physically, if the trailing edge region of the slider is lifted upward by an increased pressure force, the slider pitches forward, thereby decreasing the pitch angle.

A large change in minimum fly height with ABS temperature affects the read/write transducer operation; the transducers are located at the minimum fly height location and sensitive to the physical spacing. However, the minimum fly height change should not affect the focus of the laser beam that heats the disk. The wavelength of the laser will be greater than 100nm, which is much larger than the < 5 nm gap (probably closer to 2 nm) between the slider ABS and disk. Changing this gap (i.e. increasing the minimum fly height) by 5%-50%, which amounts to 0.1 - 1 nm for a minimum spacing of 2 nm, will not change the phase of the laser at the disk.

The miniscule percent change in flying attitude that results by neglecting thermal creep is numerically insignificant. Therefore thermal creep can be omitted from the governing lubrication equation; all important pressure profile effects are sufficiently captured by considering local air temperature values using the following equation:

$$\frac{d}{dX}\left[\frac{1}{\overline{\overline{T}}}\left(\Lambda_0 PH - \frac{PH^3}{\overline{\mu}}\overline{Q}_P\frac{dP}{dX}\right)\right] = 0 \tag{24}$$

The accuracy of simulation results using the generalized Reynolds equation can be improved by removing some simplifying assumptions. Realistic surface accommodation coefficients for the air bearing-slider and air bearing-gas interfaces could be used to generate more accurate Q_P and Q_T databases. The surfaces are not perfectly symmetric, so Q_C is not actually unity, and a Q_C database has to be generated. The details of the air property

variation across the air bearing could be accounted for by using Dowson's generalized Reynolds equation [23] that allows for fluid property variation across the film. In order to use Dowson's equation, the air bearing temperature profile through the film thickness would need to be estimated from simplified kinetic theory results. As realistic HAMR slider temperature and deformation profiles become available from experimental results or sophisticated thermo-mechanical modeling, simulations using these input files will be more accurate than the approximation profiles made in this paper.

6 Summary and Conclusions

In this paper, a generalized lubrication equation that accounts for the lateral variation of air temperature (and therefore its properties) is proposed as the governing equation for HAMR air bearing simulations. It was implemented using a production slider with plausible HAMR conditions. Most significantly, the steady state minimum fly height increased with increasing ABS temperature above ambient and increasing size of the hot area. Steady state pitch and roll angles were not appreciably affected. Thermal creep flow was shown to be negligible compared to the Poiseuille and Couette flows, and it can be omitted from the lubrication equation.

If the laser system design dissipates considerable heat, then the minimum fly height could increase $\mathcal{O}(1$ nm), thereby affecting the read/write transducer design and specifications. The focus of the laser on the recording bit should be unaffected since the wavelength of the laser is much larger than 2nm physical spacing between the slider ABS and disk at the laser delivery location. The laser delivery system needs to be designed in a manner to confine the appreciable heating of the slider body to as small an area as possible. ABS and read/write transducer designers for a HAMR system should be aware that heat dissipated from the laser delivery system into the slider body will also dissipate into the air bearing, increasing the minimum spacing compared with the results of an isothermal air bearing simulation.

Acknowledgments

The research presented here has been supported by the Computer Mechanics Laboratory, Department of Mechanical Engineering at University of California, Berkeley and the INSIC EHDR program.

References

[1] R. Rottmayer, S. Batra, D. Buechel, W. Challener, J. Hohlfeld, Y. Kubota, L. Li, B. Lu, C. Mihalcea, K. Mountfield, K. Pelhos, C. Peng, T. Rausch, M. Seigler, D. Weller, X. Yang, Heat-assisted magnetic recording, IEEE Transactions on Magnetics 42 (10) (2006) 2417–2421.

[2] M. Kryder, E. Gage, T. McDaniel, W. Challener, R. Rottmayer, G. Ju, Y.-T. Hsia, M. Erden, Heat assisted magnetic recording, Proceedings of the IEEE 96 (11) (2006) 1810–1835.

[3] W. Challener, C. Peng, A. Itagi, D. Karns, W. Peng, Y. Peng, X. Yang, X. Zhu, N. Gokemeijer, Y.-T. Hsia, G. Ju, R. Rottmayer, M. Seigler, Heat-assisted magnetic recording by a near-field transducer with efficient optical energy transfer, Nature Photonics 3 (2009) 220–224.

[4] L. Pan, D. Bogy, Data storage: Heat-assisted magnetic recording, Nature Photonics 3 (2009) 189–190.

[5] T. McDaniel, W. Challener, K. Sendur, Issues in heat-assisted perpendicular recording, IEEE Transactions on Magnetics 39 (4) (2003) 1972–1979.

[6] S. Fukui, R. Kaneko, Analysis of ultra-thin gas film lubrication based on linearized boltzmann equation: First report derivation of a generalized lubrication equation including thermal creep flow, ASME Journal of Tribology 110 (1988) 253–262.

[7] W. Huang, D. Bogy, A. Garcia, Three-dimensional direct simulation monte carlo method for slider air bearings, Physics of Fluids 9 (6) (1997) 1764–1769.

[8] S. Fukui, R. Kaneko, Handbook of MicroNano Tribology, 1st Edition, CRC Press Inc., 1995, Ch. 13 Molecular Gas Film Lubrication (MGL), pp. 559–604.

[9] W. Gross, L. Matsch, V. Castelli, A. Eshel, J. Vohr, M. Wildmann, Fluid Film Lubrication, John Wiley & Sons, Inc., New York, 1980.

[10] C. Cercignani, The Boltzmann Equation and Its Applications, Springer-Verlag, New York, 1988.

[11] C. Cercignani, M. Lampis, S. Lorenzani, Flow of a rarefied gas between parallel and almost parallel plates, in: Proceedings of 24th International Symposium on Rarefied Gas Dynamics, Vol. 762, American Institute of Physics, AIP Conference Proceedings, Melville, NY, 2005, pp. 719–724.

[12] S. Loyalka, Thermal transpiration in a cylindrical tube, Physics of Fluids 12 (11) (1969) 2301–2305.

[13] C. Cercignani, C. Pagani, Variational approach to boundary-value problems in kinetic theory, Physics of Fluids 9 (6) (1966) 1167–1173.

[14] C. Cercignani, A. Daneri, Flow of a rarefied gas between two parallel plates, Journal of Applied Physics 34 (12) (1963) 3504–3513.

[15] S. Loyalka, Kinetic theory of thermal transpiration and mechanocaloric effect. ii, The Journal of Chemical Physics 63 (9) (1975) 4054–4060.

[16] S. Chapman, T. Cowling, The Mathematical Theory of Non-Uniform Gases, 3rd Edition, Cambridge University Press, New York, 1970.

[17] E. H. Kennard, Kinetic Theory of Gases With an Introduction to Statistical Mechanics, McGraw-Hill, 1938.

[18] F. M. White, Fluid Mechanics, 5th Edition, McGraw-Hill, 2003.

[19] S. Lu, Numerical simulation of slider air bearings, Ph.D. thesis, University of California at Berkeley (1997).

[20] J. Bechtel, The effect of thermal creep flow in a heat assisted magnetic recording system, Master's thesis, University of California at Berkeley (2009).

[21] S. Loyalka, Kinetic theory of thermal transpiration and mechanocaloric effect. i, The Journal of Chemical Physics 55 (9) (1971) 4497–4503.

[22] A. Macleod, Chebyshev expansions for abramowitz functions, Applied Numerical Mathematics 10 (2) (1992) 129–137.

[23] D. Dowson, A generalized reynolds equation for fluid-film lubrication, International Journal of Mechanical Sciences 4 (1962) 159–170.